Elastic soft mode and charge ordering of Yb_4As_3

Terutaka Goto and Yuichi Nemoto
Graduate School of Science and Technology, Niigata University, Niigata 950-2181, Japan

Akira Ochiai
Material Science and Technology, Niigata University, Niigata 950-2181, Japan

Takashi Suzuki
Department of Physics, Tohoku University, Sendai 980-8578, Japan

(Received 16 June 1998)

The elastic constant of C_{44} in Yb_4As_3 relating to the transverse ultrasonic mode shows a pronounced softening around the structural phase transition point at $T_c = 292$ K associated with the charge ordering of Yb^{3+} and Yb^{2+} states. The group theoretical analysis leads to the charge fluctuation mode with Γ_5 symmetry coupled to the elastic strain $\varepsilon_{yz}, \varepsilon_{zx}, \varepsilon_{xy}$ of the soft C_{44} mode. In a framework of the Landau phenomenological theory for the phase transition, the order parameter $Q_{yz} = Q_{zx} = Q_{xy} \neq 0$ below T_c gives rise to the linear chain of Yb^{3+} ions among the body diagonal [111] direction as well as the trigonal distortion of $\varepsilon_{yz} = \varepsilon_{zx} = \varepsilon_{xy} \neq 0$. Furthermore, this theory explains experimental observations of the elastic softening $C_{44} = C_{44}^0 (T - T_c^0)/(T - \Theta)$ above T_c, the structural change from cubic phase of T_d^6 to trigonal phase of C_{3v}^6, and the first-order nature of the transition. [S0163-1829(99)00301-X]

I. INTRODUCTION

Rare-earth pnictide of Yb_4As_3 attracts considerable attention from its low-temperature behavior bearing resemblance to the heavy fermion system.[1,2] Even though it has extremely low carrier concentration, 0.1% hole per molecular unit, Yb_4As_3 exhibits a large specific-heat coefficient $C/T = 200$ mJ/mol K^2, and a T^2 dependence of low-temperature resistivity. A large magnetic susceptibility at low temperatures is similar to the Pauli paramagnetism. The Wilson ratio of magnetic susceptibility to the specific heat in Yb_4As_3 is close to the order of unity at low temperatures. No long-range magnetic order has been reported down to 45 mK in Yb_4As_3.[3] It was thought that these low-temperature properties of Yb_4As_3 are caused by the usual dense Kondo effect. However, extremely low carrier in Yb_4As_3 is not adequate to screen the spin freedom of the localized *4f* electron by the Kondo scenario.

Yb_4As_3 crystallizes to the anti-Th_3P_4 structure with the space group symmetry of T_d^6.[4] Two molecules of Yb_4As_3 are contained in the unit cell defined by the basic vectors $1/2(-a,a,a)$, $1/2(a,-a,a)$, $1/2(a,a,-a)$ of the Bravais lattice of the body-centered cubic Γ_c^v. The magnetic susceptibility,[1] Mössbauer spectroscopy[3] and perturbed angular correlation of ^{127}Yb ions[5] indicate that Yb^{3+} ions with the $4f^{13}$ configuration and Yb^{2+} ions with the closed $4f^{14}$ shell coexist in the ratio of 1 to 3. This mixed valence state is consistent with charge neutrality of $Yb^{3+}(Yb^{2+})_3(As^{3-})_3$. The structural phase transition from cubic phase with the space group T_d^6 to the trigonal phase with C_{3v}^6 occurs at $T_c = 292$ K.[1,6] The absence of the superlattice in the x-ray measurement below structural transition point shows the volume of the unit cell to be conserved in the charge ordering around $T_c = 292$ K. The tiny deviation from the orthogonal axes in the cubic phase to an angle of $\alpha = 90.8°$ in the trigonal phase means the spontaneous elastic strain of $\varepsilon_{yz} = \varepsilon_{zx} = \varepsilon_{xy} \neq 0$ below T_c.[4,7] The abrupt change of the angle α at the structural transition point indicates the first-order nature of the phase change at $T_c = 292$ K.

The hole orbit $4f^{13}$ in the trivalent Yb^{3+} ion has the ground state of the magnetic multiplet with $J = 7/2$, $L = 3$, $S = 1/2$, while the closed shell $4f^{14}$ in divalent Yb^{2+} is characterized by the nonmagnetic ground state of $J = 0$, $L = 0$, $S = 0$. Under applied external magnetic field, therefore, one can detect an induced magnetic moment of Yb^{3+} ions even in the paramagnetic state. Recently Kohgi *et al.* performed a skillful experiment by the polarized neutron scattering under magnetic fields and detected the induced magnetic moment of Yb^{3+} ions aligned along the [111] direction parallel to the uniaxial external stress field in the charge-ordered phase below T_c.[8] Furthermore, the neutron experiments observed the one-dimensional excitation of the Yb^{3+} linear chain with the antiferro-Heisenberg exchange interaction. Recently Fulde and co-workers[9–11] proposed a one-dimensional band Jahn-Teller model for the linear chain of Yb^{3+} ions, which explains the heavy-Fermion behavior of large specific heat in Yb_4As_3 at low temperatures. The charge freedom of the 4*f* holes of Yb^{3+} ions in the sea of Yb^{2+} ions with the Coulomb interaction leads to the charge ordering of Yb_4As_3. The spin freedom of $4f^{13}$ in the Yb^{3+} ion gives rise to the one-dimensional magnetism at low temperatures. The interplay of charge and spin freedoms is the central issue for the unusual properties in Yb_4As_3. The optical[12,13] and cyclotron resonance[14] measurements have been done to elucidate the origin of the low carrier in Yb_4As_3. The energy-band calculation of Yb_4As_3 shows the valence instability and the *4f* hole near the Fermi level indicating the low-carrier behavior of the system.[15–17] The influence of the hole carrier to the

charge order and one-dimensional magnetism in Yb_4As_3 is still an open problem.

In the present paper we have performed the ultrasonic measurement to examine the elastic properties in Yb_4As_3. The experimental procedure is presented in Sec. II and the result of the ultrasonic measurements in Sec. III. We describe the Landau phenomenological theory to explain the charge ordering in Yb_4As_3 in Sec. IV. In Sec. V we discuss the character of charge fluctuation mode and the charge ordering in Yb_4As_3.

II. EXPERIMENT

The single crystal of Yb_4As_3 was grown in a W crucible sealed by an electron-beam technique. Because the phase of Yb_4As_3 melts incongruently, the single phase of Yb_4As_3 was grown inside the W crucible with temperature gradient by a high-frequency electrical furnace. The crystallographic orientation of Yb_4As_3 was determined by the x-ray photograph. The sample with rectangular shape of $2\times3\times4$ mm^3 for the ultrasonic measurement was prepared by an electrical spark cutter. In order to observe the ultrasonic pulse echoes with an exponential decay, we polished carefully the surfaces of samples to be parallel. The $LiNbO_3$ transducers for the generation and detection of the sound waves with the frequencies 10–50 MHz were bonded on the surfaces of the sample. The sound-wave velocity v was detected by an ultrasonic apparatus based on the phase-comparison method. In the estimation of the elastic constant $C=\rho v^2$, we used the mass density $\rho=8.98$ g/cm^3 from the lattice constant $a=8.788$ Å of the present sample of Yb_4As_3.

III. RESULTS

We show the temperature dependence of the elastic constants C_{ij} of Yb_4As_3 in Fig. 1. The elastic constant of C_{44}, which was measured by the transverse mode propagating along the [100] axis with the polarization vector parallel to the [001] axis, shows a pronounced softening below 400 K down to the phase transition point $T_c=292$ K.[18] The ultrasonic echo signal disappears abruptly below T_c due to the strong increase of the ultrasonic attenuation associated with the elastic domain. An increase of the elastic constant C_{44} is observed in lowering temperature in the ordered phase. The elastic softening of C_{44} in Fig. 1 suggests that the elastic strain $\varepsilon_{yz},\varepsilon_{zx},\varepsilon_{xy}$ with Γ_5 symmetry of the C_{44} mode plays the main role for the charge ordering in Yb_4As_3. We present a mechanism of the charge ordering in Sec. IV. On the other hand, the transverse $(C_{11}-C_{12})/2$ mode propagating along the [110] axis with the polarization parallel to [110] shows only a steplike anomaly at T_c. This result means that the $(C_{11}-C_{12})/2$ mode characterized by the elastic strain of $\varepsilon_u=(2\varepsilon_{zz}-\varepsilon_{xx}-\varepsilon_{yy})/\sqrt{3}$ or $\varepsilon_v=\varepsilon_{xx}-\varepsilon_{yy}$ with Γ_3 symmetry does not contribute for the charge ordering in Yb_4As_3.

The elastic constant C_{11} corresponding to the longitudinal ultrasonic mode propagating along the [100] axis also exhibits a discontinuity at T_c. Furthermore, the bulk modulus C_B $(C_{11}+2C_{12})/3$ associated with the volume strain $\varepsilon_B=\varepsilon_{xx}+\varepsilon_{yy}+\varepsilon_{zz}$ with Γ_1 symmetry shows a small step at T_c and increases slightly in lowering temperature. The bulk modulus C_B of Yb_4As_3 in Fig. 1 was calculated by the experimental

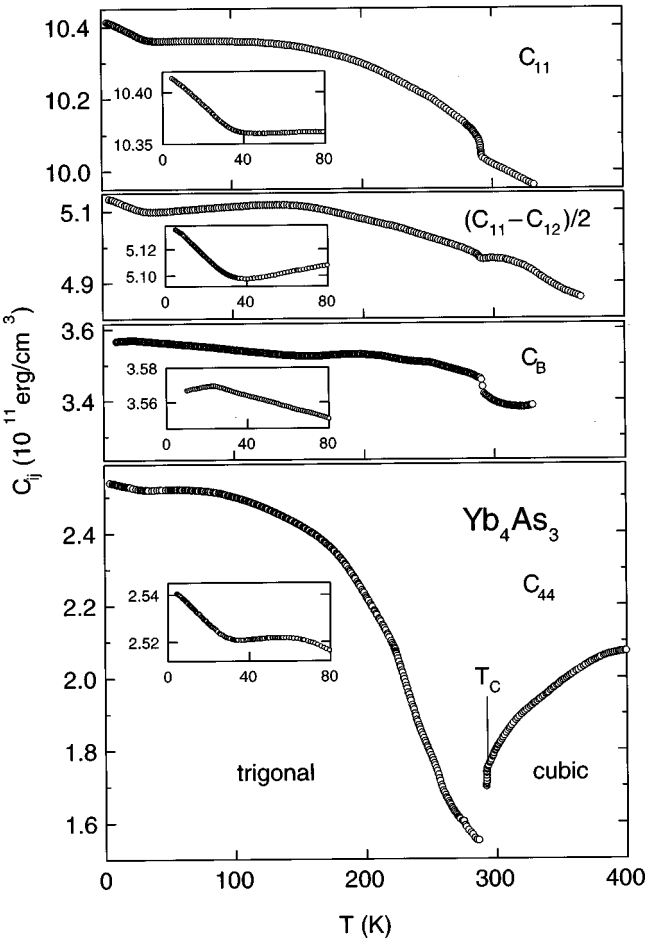

FIG. 1. Temperature dependence of the elastic constants in the mixed-valence compound Yb_4As_3. The elastic softening of the transverse C_{44} mode has been found around the structural phase transition point $T_c=292$ K from cubic phase T_d^6 to trigonal phase C_{3v}^6 associated with the charge ordering. Insets show low-temperature anomalies of the elastic constants in the ordered phase with the trigonal lattice in Yb_4As_3.

results of C_{11} and $(C_{11}-C_{12})/2$. This normal behavior of C_B in Yb_4As_3 is considerable contrast to the softening of C_B in the intermediate-valence compound SmB_6.[19] The softening of C_B in SmB_6 means the Sm^{2+} ions changes easily into Sm^{3+} ions with relatively small ionic radius as the volume of the crystal shrinks with the external hydrostatic pressure. In the present case of Yb_4As_3, however, the absence of the softening of C_B implies that the coexistence ratio of Yb^{3+} and Yb^{2+} ions is conserved to be 1 to 3 even at the charge-ordering point $T_c=292$ K. In the Landau theory in the next section, therefore, we include the bilinear coupling of the charge fluctuation mode with Γ_5 symmetry to the elastic C_{44} mode in the free-energy density, but the coupling of the charge fluctuation mode of Γ_1 to the volume strain ε_B is excluded.

The low-temperature behavior of the elastic constants of Yb_4As_3 is shown in insets of Fig. 1 in expanded scales. The shallow minimums around 40 K are found commonly in the elastic constants of C_{11}, $(C_{11}-C_{12})/2$, and C_{44}. The bulk modulus C_B, however, exhibits monotonous increase at low temperatures. The $4f^{13}$ state in Yb^{3+} ions has both spin and

orbital degrees of freedom. The crystalline electric fields (CEF) with trigonal symmetry below T_c splits the ground-state multiplet of $J=7/2$ into four Kramers doublets.[8] The quadrupolar moments of the CEF state in Yb_4As_3 may couple to the elastic strains of the $(C_{11}-C_{12})/2$ and C_{44} modes. The low-temperature anomalies in Fig. 1, therefore, may be explained by the quadrupolar susceptibility for the CEF state of $J=7/2$ of Yb^{3+} due to the quadrupolar-strain interaction. In the present paper we focus the elastic soft mode C_{44} due to the charge ordering. The coupling of the quadrupolar moment of the $4f$-hole state $4f^{13}$ in the linear chain of Yb^{3+} ions along the [111] direction to the elastic strain remains an unresolved problem in ultrasonic experiments of Yb_4As_3.

IV. ANALYSIS

As presented in the previous section, the softening of the elastic constant C_{44} in Yb_4As_3 is the most striking feature of the structural phase transition associated with the charge ordering. Various physical quantities like the elastic constants in Sec. III show the discontinuous change at the transition point $T_c=292$ K. This means the phase transition of Yb_4As_3 is first order. The Landau theory is based on the second-order transition associated with the continuous change of the order parameter at the transition point. Even though there is a first-order nature of the charge ordering in Yb_4As_3, it is of great significant to employ the Landau theory for the phase transition where the group-subgroup relation is expected. In this section we make the group-theoretical analysis to project the charge-fluctuation mode, which freezes at the charge-ordering point T_c. Furthermore, we construct the Gibbs free-energy density described by the order parameter of the charge ordering.

In Fig. 2, we show a conventional unit cell of Yb_4As_3 with the anti-Th_3P_4 structure of the space group $T_d^6(I43d)$. It should be noted that the conventional unit cell in Fig. 2 consisting of 16 Yb atoms and 12 As atoms is chosen to follow the conventional crystallographic axes. Therefore, the volume of the conventional unit cell in Fig. 2 is twice as large as the unit cell of the Bravais lattice Γ_c^v. The nonsymmorphic space group T_d^6 has 24 symmetry operators $\{\boldsymbol{R}|\boldsymbol{b}\}$, where both rotation $\boldsymbol{R}$ and nonprimitive translation $\boldsymbol{b}$ are included. We refer to the definite presentation of the operators $\{\boldsymbol{R}|\boldsymbol{b}\}$ for the space group T_d^6 that can be found in *International Tables for Crystallography*.[20] In the present analysis we assume that Yb^{3+} and Yb^{2+} ions coexist in the ratio of 1 to 3 and exhibit thermal fluctuation around the mean valence of 2.25+. This conjecture of the charge neutrality in Yb_4As_3 seems to be reasonable because of the extremely low carrier concentration of 0.1% per unit molecule. The effect of the relative displacement of $Yb^{3+}$and Yb^{2+} ions with respect to As^{3-} ions is omitted. The lack of the inversion symmetry in the present compound Yb_4As_3 with the space group T_d^6 leads to the piezoelectric character of the crystal. The relative displacement of Yb ions with respect to As ions could play an important role for the dielectric properties of Yb_4As_3.

We introduce the charge density ρ_i $(i=1,2\ \ldots\ ,8)$ as a function of the position vector for the ith site of the Yb ion in Fig. 2 as

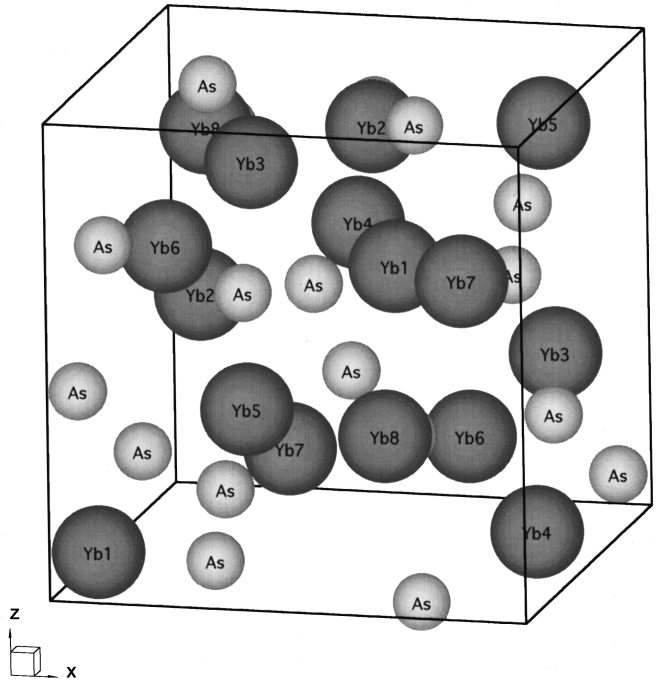

FIG. 2. Conventional unit cell of Yb_4As_3 with the anti-Th_3P_4 structure of space group T_d^6. The unit cell involves four chemical formulas of Yb_4As_3. Because of the body-centered symmetry of the crystal, there are eight Yb sites with the crystallographic independence.

$$
\begin{aligned}
&\text{Yb1:}\ \ \rho_1=\rho_1(u,u,u),\\
&\text{Yb2:}\ \ \rho_2=\rho_2(u,-u,-u+1/2),\\
&\text{Yb3:}\ \ \rho_3=\rho_3(-u+1/2,u,-u),\\
&\text{Yb4:}\ \ \rho_4=\rho_4(-u,-u+1/2,u),\\
&\text{Yb5:}\ \ \rho_5=\rho_5(u+1/4,u+1/4,u+1/4),\\
&\text{Yb6:}\ \ \rho_6=\rho_6(-u+1/4,u+1/4,-u+3/4),\\
&\text{Yb7:}\ \ \rho_7=\rho_7(u+1/4,-u+3/4,-u+1/4),\\
&\text{Yb8:}\ \ \rho_8=\rho_8(-u+3/4,-u+1/4,u+1/4).
\end{aligned}
\qquad (1)
$$

bc

In the present compound of Yb_4As_3, the parameter in the charge density of Eq. (1) is $u=0.069$ in unit of the lattice parameter.[4] Because of the body-centered (bc) symmetry of the present crystal, there are two equivalent sites for Yb ions in the conventional unit cell of Fig. 2, which are connected with the pure translation operator of $\{\boldsymbol{E}|1/2\ 1/2\ 1/2\}$ each other. In the group-theoretical analysis, therefore, it is sufficient to consider charge density ρ_i $(i=1,2,\ \ldots\ ,8)$ for 8 Yb sites in Fig. 2. When 24 symmetry operators of space group T_d^6 act on ρ_i $(i=1,2,\ \ldots\ ,8)$, one gets the representation matrix with 8×8 elements. The character for the charge density of ρ_i $(i=1,2,\ \ldots\ ,8)$ obtained by the trace for representation matrix is decomposed into a direct sum of the irreducible representations $\Gamma_1(1D)\oplus\Gamma_2(1D)\oplus\Gamma_4(3D)\oplus\Gamma_5(3D)$. Consequently there are charge-fluctuation modes with Γ_5

TABLE I. The bases of the charge-fluctuation modes in the high-temperature phase with space group T_d^6 in Yb_4As_3. The triplet state of the charge-fluctuation mode $\rho_{\Gamma5,yz}, \rho_{\Gamma5,zx}, \rho_{\Gamma5,xy}$ couples to the elastic strain $\varepsilon_{yz}, \varepsilon_{zx}, \varepsilon_{xy}$ of the soft elastic C_{44} mode. The coupling of the full symmetry mode $\rho_{\Gamma1}$ to the volume strain $\varepsilon_B = \varepsilon_{xx} + \varepsilon_{yy} + \varepsilon_{zz}$ does not play an important role in the charge ordering in Yb_4As_3.

Symmetry	Charge-fluctuation mode	Elastic strain
Γ_1	$\rho_{\Gamma1} = \rho_1 + \rho_2 + \rho_3 + \rho_4 + \rho_5 + \rho_6 + \rho_7 + \rho_8$	$\varepsilon_B = \varepsilon_{xx} + \varepsilon_{yy} + \varepsilon_{zz}$
Γ_2	$\rho_{\Gamma2} = \rho_1 + \rho_2 + \rho_3 + \rho_4 - \rho_5 - \rho_6 - \rho_7 - \rho_8$	
Γ_3		$\varepsilon_u = (2\varepsilon_{zz} - \varepsilon_{xx} - \varepsilon_{yy})/\sqrt{3}$
		$\varepsilon_v = \varepsilon_{xx} - \varepsilon_{yy}$
Γ_4	$\rho_{\Gamma4,x} = \rho_1 + \rho_2 - \rho_3 - \rho_4 - \rho_5 + \rho_6 - \rho_7 + \rho_8$	
	$\rho_{\Gamma4,y} = \rho_1 - \rho_2 + \rho_3 - \rho_4 - \rho_5 - \rho_6 + \rho_7 + \rho_8$	
	$\rho_{\Gamma4,z} = \rho_1 - \rho_2 - \rho_3 + \rho_4 - \rho_5 + \rho_6 + \rho_7 - \rho_8$	
Γ_5	$\rho_{\Gamma5,yz} = \rho_1 + \rho_2 - \rho_3 - \rho_4 + \rho_5 - \rho_6 + \rho_7 - \rho_8$	ε_{yz}
	$\rho_{\Gamma5,zx} = \rho_1 - \rho_2 + \rho_3 - \rho_4 + \rho_5 + \rho_6 - \rho_7 - \rho_8$	ε_{zx}
	$\rho_{\Gamma5,xy} = \rho_1 - \rho_2 - \rho_3 + \rho_4 + \rho_5 - \rho_6 - \rho_7 + \rho_8$	ε_{xy}

symmetry, which will couple to the elastic strains $\varepsilon_{yz}, \varepsilon_{zy}, \varepsilon_{xy}$ of the soft elastic C_{44} mode. The lack of Γ_3 representation in the charge-fluctuation modes is in agreement with the absence of the elastic softening around T_c in the $(C_{11}-C_{12})/2$ mode associated with the $\varepsilon_v = \varepsilon_{xx} - \varepsilon_{yy}$ strain of Γ_3 symmetry. There is a charge-fluctuation mode with full symmetry of Γ_1. However, the absence of the elastic softening in the bulk modulus C_B in Fig. 1 associated with the strain $\varepsilon_B = \varepsilon_{xx} + \varepsilon_{yy} + \varepsilon_{zz}$ of Γ_1 implies that the charge fluctuation of Γ_1 is stable even around T_c.

The projection operator[21] derives the bases of the irreducible representations consisting of linear combination of the charge density ρ_i $(i = 1,2, \ldots, 8)$ for the Yb sties. The bases of the irreducible representations are listed in Table I. The basis of $\rho_{\Gamma1} = \rho_1 + \rho_2 + \rho_3 + \rho_4 + \rho_5 + \rho_6 + \rho_7 + \rho_8$ means the thermal distribution of the *4f* holes associated with two Yb^{3+} ions to the 8 Yb sites in Fig. 1 with equal weight. This mode of $\rho_{\Gamma1}$ corresponds to a uniform charge distribution with the mean valence 2.25+. Other bases of $\rho_{\Gamma2}$, $\rho_{\Gamma4}$, and $\rho_{\Gamma5}$ with the symmetry-breaking character in Table I indicate the charge-fluctuation modes with anisotropic charge distributions.

In the Landau theory for the phase transition, the Gibbs free energy is explained by the function of the atom or electron density $\rho = \rho(x,y,z)$.[22] Here x,y,z mean the coordinate of the atom or electron. In the present case the function $\rho(x,y,z)$ means the charge density for the *4f* hole of $4f^{13}$ in Yb^{3+} in the sea of Yb^{2+} ions in crystal. The modulation of charge density involving the charge ordering is written as $\rho = \rho_0 + \Delta\rho$. Here ρ_0 is the charge-density part that is invariant across the phase transition point. Therefore ρ_0 is expanded by the basis with full symmetry Γ_1 of space group T_d^6 in the high-temperature phase above T_c. The second term $\Delta\rho$ is due to the symmetry-breaking part, which changes at the charge-ordering point T_c. This means that $\Delta\rho = 0$ in the high-symmetry phase above T_c and $\Delta\rho \neq 0$ in the low-symmetry phase below T_c.

In the present case of Yb_4As_3, $\Delta\rho$ is expanded by the charge-fluctuation mode $\rho_{\Gamma5,yz}, \rho_{\Gamma5,zx}, \rho_{\Gamma5,xy}$ with Γ_5 symmetry in Fig. 3. This mode is quenched at the charge-ordering point T_c.

$$\Delta\rho = \Sigma_\gamma Q_\gamma \rho_{\Gamma5,\gamma} = Q_{yz}\rho_{\Gamma5,yz} + Q_{zx}\rho_{\Gamma5,zx} + Q_{xy}\rho_{\Gamma5,xy}. \tag{2}$$

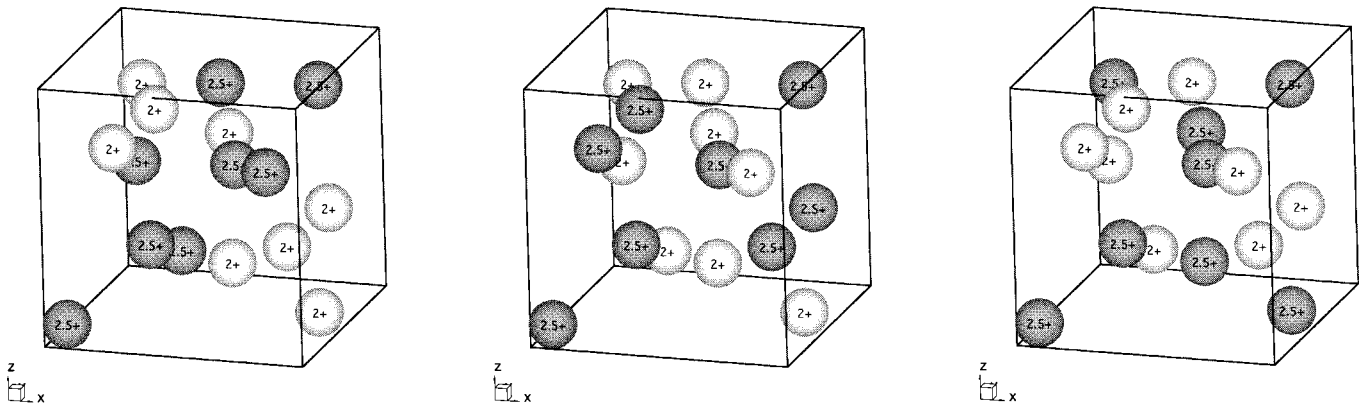

$\rho_{\Gamma5,yz}$ $\rho_{\Gamma5,zx}$ $\rho_{\Gamma5,xy}$

FIG. 3. The charge fluctuation mode of $\rho_{\Gamma5,yz}, \rho_{\Gamma5,zx}, \rho_{\Gamma5,xy}$ with Γ_5 symmetry is quenched at the charge-ordering point $T_c = 292$ K in Yb_4As_3. The valence of 2.5+ in figure means that the $4f^{13}$ hole of Yb^{3+} ion thermally populates on the Yb site with half-weight. The valence of 2.0+ in the figure indicates the Yb^{2+} ion on the site.

Here the coefficients Q_{yx}, Q_{zx}, Q_{xy} in Eq. (2) are the order parameter to describe the charge ordering of Yb_4As_3. The order parameter Q_{yz}, Q_{zx}, Q_{xy} should be zero in the high-temperature phase above T_c. In principle we can expect three possibilities for the ordered phase: (i) $Q_{yz} \neq 0$, $Q_{zx} = Q_{xy} = 0$, (ii) $Q_{yz} = Q_{zx} \neq 0$, $Q_{xy} = 0$, (iii) $Q_{yz} = Q_{zx} = Q_{xy} \neq 0$. It is of great interest to consider the last case of (iii), which leads to the ordered phase with the space-group symmetry C_{3v}^6 of the trigonal lattice. The space group C_{3v}^6 is the subgroup of T_d^6 in the high-temperature phase. The present analysis confirms the trigonal lattice with the space group C_{3v}^6 below T_c in Yb_4As_3 by the electron-microscope experiment.[1]

When the body-diagonal [111] direction is chosen to be a unique axis of the trigonal lattice of C_{3v}^6 in the low-temperature phase, one can find the charge density $\Delta\rho_{\text{order}}$, which appears in the charge-ordered phase far below T_c. At low temperatures one can expect the order parameter Q_{ij} $(i,j=x,y,z, i \neq j)$ in Eq. (2) to be unity.

$$\Delta\rho_{\text{order}} = \rho_{\Gamma 5,yz} + \rho_{\Gamma 5,zx} + \rho_{\Gamma 5,xy} = 3\rho_1 - \rho_2 - \rho_3 - \rho_4 + 3\rho_5 - \rho_6 - \rho_7 - \rho_8. \quad (3)$$

The six symmetry operators of the space group C_{3v}^6 keep the charge density $\Delta\rho_{\text{order}}$ of Eq. (3) invariant. This means that the charge-fluctuation mode of $\rho_{\Gamma 5,yz} + \rho_{\Gamma 5,zx} + \rho_{\Gamma 5,xy}$ in Fig. 4 is the active representation of space group T_d^6 for the transition of the C_{3v}^6 phase.

In the high-temperature phase above T_c, the charge e due to the *4f* hole of the Yb^{3+} ion is thermally distributed in the sea of Yb^{2+} ions. In the case of the charge-fluctuation mode $\rho_{\Gamma 5,yz}, \rho_{\Gamma 5,zx}, \rho_{\Gamma 5,xy}$ in Fig. 3, the charge distribution is not uniform, but locates the peculiar Yb sites with half-weight of charge $e/2$. The charge fluctuation mode $\rho_{\Gamma 5,yz}$ in Fig. 3, for example, leads to the intermediate valence of 2.5+ for the sites of Yb1, Yb2, Yb5, Yb7, while the absence of the *4f* hole means the valence of 2.0+ for the sites of Yb3, Yb4, Yb6, Yb8. It should be noted that when we measure the distance from the Yb1 site, Yb2, Yb3, Yb4 sites are located at the first nearest neighbor, Yb5 corresponds to the second-nearest neighbor, and Yb6, Yb7, Yb8 locate at the third nearest neighbor. It is expected that the *4f* hole of the Yb^{3+} ion in Yb_4As_3 localizes well on the Yb site. In the ordered phase, therefore, the charge distribution of half-weight with the charge $e/2$ is expected to be unstable, and only the localized state of the $4f$ hole with unit charge e is available at low temperatures. This simple principle promises that the two types of the ordered phases corresponding to (i) $Q_{yz} \neq 0$, $Q_{zx} = Q_{xy} = 0$ and (ii) $Q_{yz} = Q_{zx} \neq 0$, $Q_{xy} = 0$ are not stable at low temperatures. The ordered phase for (iii) $Q_{yz} = Q_{zx} = Q_{xy} \neq 0$ seems to be stable because the charge ordering with unit charge e is available. As one can see in Fig. 4, the charge density $\Delta\rho_{\text{order}}$ of Eq. (3) corresponds to the linear alignment of the *4f* hole with unit charge e along the body-diagonal direction [111]. This arrangement of the charge density $\Delta\rho_{\text{order}}$ is actually realized in the ordered phase below $T_c = 292$ K in Yb_4As_3.

The structural change from the high-temperature cubic phase of T_d^6 to the low-temperature trigonal phase of C_{3v}^6 is accompanied by the charge ordering in Yb_4As_3. The elastic

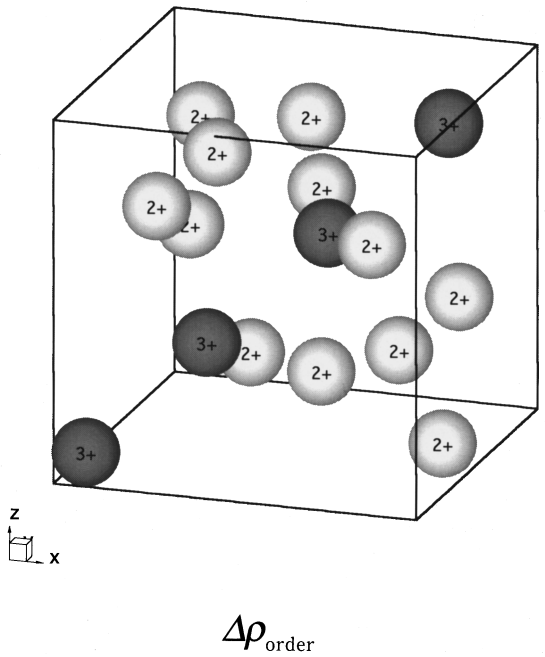

FIG. 4. The charge-ordered structure of $\Delta\rho_{\text{order}} = \rho_{\Gamma 5,yz} + \rho_{\Gamma 5,zx} + \rho_{\Gamma 5,xy}$ in the low-temperature phase of C_{3v}^6 in Yb_4As_3. The *4f* hole of the Yb^{3+} ion aligns along the body-diagonal [111] direction.

softening of the transverse C_{44} mode around the charge-ordering point has been found in the present ultrasonic experiment. In order to describe the lattice instability due to the charge ordering, it is useful to consider the free-energy density F expanded by the power series of the order parameter Q_{yz}, Q_{zx}, Q_{xy} as well as the elastic strain $\varepsilon_{yz}, \varepsilon_{zx}, \varepsilon_{xy}$ of the C_{44} mode.[23]

$$F = F_0 + \tfrac{1}{2}\alpha(Q_{yz}^2 + Q_{zx}^2 + Q_{xy}^2) + \tfrac{1}{3}\beta Q_{yz}Q_{zx}Q_{xy} + \tfrac{1}{4}\gamma[Q_{yz}^4 + Q_{zx}^4 + Q_{xy}^4 - \tfrac{3}{5}(Q_{yz}^2 + Q_{zx}^2 + Q_{xy}^2)^2] + \delta(Q_{yz}\varepsilon_{yz} + Q_{zx}\varepsilon_{zx} + Q_{xy}\varepsilon_{xy}) + \tfrac{1}{2}C_{44}^0(\varepsilon_{yz}^2 + \varepsilon_{zx}^2 + \varepsilon_{xy}^2). \quad (4)$$

Here F_0 is a part free from the phase transition. Because the inversion symmetry does not exist in the space group T_d^6 of the high-temperature phase in Yb_4As_3, the bases of $\{yz, zx, xy\}$ as well as $\{x, y, z\}$ belong to the same irreducible representation Γ_5. In the free-energy density of Eq. (4) in the present case, therefore, the third-order power of $(\tfrac{1}{3})\beta Q_{yz}Q_{zx}Q_{xy}$ is also an invaraint term in addition to odd powers of order parameter and elastic strain. This third-order term in the cubic crystal without inversion symmetry gives rise to the first-order phase transition.

The order parameters Q_{yz}, Q_{zx}, Q_{xy} due to the charge-fluctuation mode in Fig. 3 are characterized by the wave vector $\boldsymbol{q} = 0$ at the Brillouin zone center Γ point. Therefore the bilinear coupling of Q_{yz}, Q_{zx}, Q_{xy} to the elastic strain with $\boldsymbol{q} = 0$ in Eq. (4) is available. The charge ordering will be realized at the Brillouin zone center Γ point. This argument is consistent with the x-ray measurement, where the superlattice is not observed below $T_c = 292$ K in Yb_4As_3. In the higher-order term, the order parameters may couple quadratically to the elastic strain in principle. This quadratic coupling

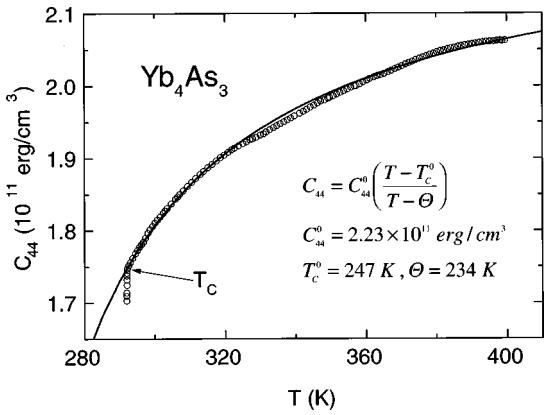

FIG. 5. The elastic softening of the transverse C_{44} mode in the high-temperature phase of space group T_d^6 in Yb_4As_3. The bilinear coupling term of the charge-fluctuation mode $\rho_{\Gamma5,yz},\rho_{\Gamma5,zx},\rho_{\Gamma5,xy}$ in Fig. 3 to the elastic strains $\varepsilon_{yz},\varepsilon_{zx},\varepsilon_{xy}$ of the C_{44} mode leads to the elastic soft mode of $C_{44}=C_{44}^0(T-T_c^0)/(T-\Theta)$ for $T>T_c$. The solid line in the figure is a fit with the parameters $T_c^0=247$ K, $\Theta=234$ K, and $C_{44}^0=2.23\times10^{11}$ ergs/cm^3.

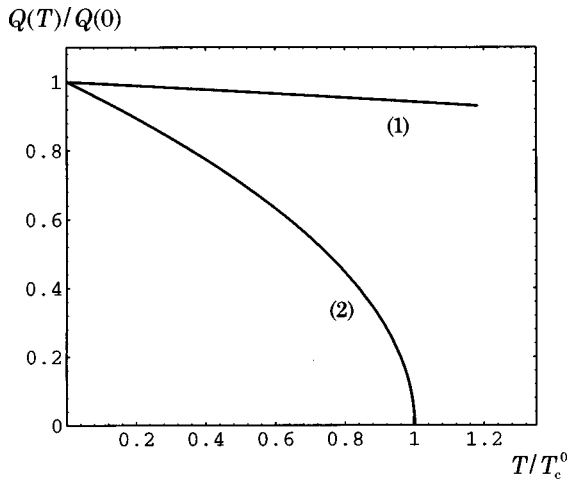

FIG. 6. The temperature dependence of the order parameter $Q(T)$ for the charge ordering below T_c. Case (2) indicates the second-order transition with $\beta=0$ in the free energy. Case (1) means the first-order transition with the parameters of $A=(-5\alpha_0/4\gamma)=0.20$ and $B=(-5\beta/12\gamma)=-1.74$. The temperature dependence of the trigonal angle indicated by the x-ray measurement in Ref. 7 is reproduced by the present calculation with $\delta=-1.56\times10^9$ ergs/cm^3 in Eq. (9).

gives rise to a jump at the transition point but does not explain the elastic softening in C_{44} of Yb_4As_3. Therefore we consider only the bilinear coupling term in Eq. (4).

We assume that the coefficient α of the second-order power in Eq. (4) passes through zero at a characteristic temperature Θ as $\alpha=\alpha_0(T-\Theta)$. In the present case the charge-fluctuation mode $\rho_{\Gamma5,yz},\rho_{\Gamma5,zx},\rho_{\Gamma5,xy}$ in Fig. 3 gives rise to the Coulomb interaction among unit cells at different sites. It is expected that the quadrupolar interaction in the lowest order plays a main role in providing the temperature Θ in the coefficient α. The fourth-order term in Eq. (4) is necessarily positive because of the stability of the system. The bilinear coupling of the order parameter to the elastic strain in Eq. (4) gives rise to the structural phase transition associated with the charge ordering. The elastic constant C_{44}^0 in the elastic energy term in Eq. (4) means the stiffness in the absence of the coupling of the elastic strain to the charge-fluctuation mode $\rho_{\Gamma5,yz},\rho_{\Gamma5,zx},\rho_{\Gamma5,xy}$.

By use to the stability condition $\partial F/\partial Q_{ij}=0$ $(i,j=x,y,z,\ i\neq j)$, one gets the renormalized elastic energy in the high-temperature phase as

$$\tilde{F}=F_0+\frac{1}{2}\left(C_{44}^0-\frac{\delta^2}{\alpha}\right)(\varepsilon_{yz}^2+\varepsilon_{zx}^2+\varepsilon_{xy}^2). \tag{5}$$

The second derivative of the renormalized free-energy equation (5) with respect to the elastic strain provides the elastic constant C_{44} in the high-temperature phase.

$$C_{44}=\frac{\partial^2\tilde{F}}{\partial\varepsilon_{ij}^2}=C_{44}^0\left(\frac{T-T_c^0}{T-\Theta}\right)\quad(i,j=x,y,z,i\neq j). \tag{6}$$

Here the critical temperature T_c^0 corresponding to the elastic instability point for the second-order transition is written as $T_c^0=\Theta+(\delta^2/\alpha_0C_{44}^0)$. In the present case of Yb_4As_3, however, the third-order term in Eq. (4) gives rise to the first-order transition at T_c, which is higher than T_c^0.

In Fig. 5 we show the elastic softening of the transverse C_{44} mode in the high-temperature phase of Yb_4As_3. The solid line in Fig. 5 is a fit by the formula of the elastic constant of Eq. (6) with parameters $T_c^0=247$ K, $\Theta=234$ K, and $C_{44}^0=2.23\times10^{11}$ ergs/cm^3. The experimental observation of the transition point $T_c=292$ K in the present crystal of Yb_4As_3 is considerably higher than the critical temperature of $T_c^0=247$ K. This result implies the first-order phase transition of the charge ordering in Yb_4As_3. The difference between $T_c^0=247$ K and $\Theta=234$ K is the coupling energy $\delta^2/\alpha_0C_{44}^0=13$ K between the charge-fluctuation mode and the elastic strain of the C_{44} mode.

The temperature dependence of the order parameter below T_c is also explained by the free-energy density of Eq. (4). Concerning the trigonal distortion below T_c, we take $Q_{yz}=Q_{zx}=Q_{xy}=Q$ in Eq. (4).

$$\tilde{F}=F_0+\frac{3}{2}\left(\alpha-\frac{\delta^2}{C_{44}^0}\right)Q^2+\frac{1}{3}\beta Q^3-\frac{3}{5}\gamma Q^4. \tag{7}$$

The stability condition requires a positive value of the fourth-order term ($\gamma<0$) in Eq. (7). The minimum condition of the free-energy density of Eq. (7) leads to the equation for the order parameter written as

$$3\alpha_0(T-T_c^0)Q+\beta Q^2-\tfrac{12}{5}\gamma Q^3=0. \tag{8}$$

The solution of $Q=0$ means the high-temperature phase above T_c. In the case of the second-order transition for $\beta=0$ in Eq. (8), the temperature dependence of the order parameter below T_c is written as $Q=Q_0[(T_c^0-T)/T_c^0]^{1/2}$. Here the amplitude is defined as $Q_0=(-5/4)^{1/2}(\alpha_0T_c^0/\gamma)^{1/2}$. The continuous change of the order parameter is presented in case (2) in Fig. 6. The first-order transition accompanied by the discontinuous change of the order parameter is shown in case (1) in Fig. 6, where the parameters of $A=(-5\alpha_0/4\gamma)=0.20$ and $B=(-5\beta/12\gamma)=-1.74$ are assumed.

The stability condition for the free-energy density of Eq. (4), $\partial F/\partial \varepsilon_{ij}=0$ $(i,j=x,y,z,\ i\neq j)$, provides the spontaneous strain proportional to the order parameter below T_c,

$$\varepsilon_{ij}=-\frac{\delta}{C_{44}^0}Q_{ij} \quad (i,j=x,y,z,\ i\neq j). \tag{9}$$

The angle $\alpha=90°+2\theta$ in the trigonal phase distorted from the orthogonal axes in the cubic phase is related to the spontaneous elastic strain proportional to the order parameter below T_c.

$$\varepsilon_{ij}=\sin\theta \quad (i,j=x,y,z,\ i\neq j). \tag{10}$$

The x-ray measurement of Yb_4As_3 showed a discontinuous change of the angle from $\alpha=90°$ to $\alpha=90.74°$ ($\theta=0.37°$) at $T_c=292$ K.[7] According to Eq. (10), one gets the spontaneous strain $\varepsilon_{yz}=\varepsilon_{zx}=\varepsilon_{xy}=6.46\times10^{-3}$ at T_c leading to the trigonal distortion with the principal axis along [111]. We have already calculated case (1) in Fig. 6 corresponding to the discontinuous change of the order parameter at T_c. In taking the coupling parameter $\delta=-1.56\times10^9$ ergs/cm^3 in Eq. (9), the temperature dependence of the order parameter of case (1) in Fig. 6 reproduces successfully the trigonal distortion below T_c in Yb_4As_3 by the x-ray measurement.[7] The negative sign of the coupling constant δ leads to the linear chain of Yb^{3+} ions along the [111] direction being shrunk below T_c. This is consistent with the ionic radii of Yb^{3+} ion to be smaller than that of the Yb^{2+} ion.

V. CONCLUDING REMARKS

In the present paper we show the elastic softening of the transverse C_{44} mode around the charge-ordering point in Yb_4As_3. We introduce the bilinear coupling mechanism of the elastic strain $\varepsilon_{yz},\varepsilon_{zx},\varepsilon_{xy}$ of the C_{44} mode with Γ_5 symmetry to the charge-fluctuation mode with Γ_5 symmetry. We employ the group-theoretical analysis to pick up the charge-fluctuation mode of Yb^{3+} ions in the sea of Yb^{2+} ions in the high-temperature cubic phase with the space group T_d^6. The charge-fluctuation modes are decomposed into irreducible representations Γ_1, Γ_2, Γ_4, and Γ_5. The bilinear coupling between the charge-fluctuation mode $\rho_{\Gamma5,yz},\rho_{\Gamma5,zx},\rho_{\Gamma5,xy}$ and the elastic strain $\varepsilon_{yz},\varepsilon_{zx},\varepsilon_{xy}$ gives rise to the structural phase transition from the cubic phase of T_d^6 to the trigonal phase of C_{3v}^6. This mechanism of structural change resembles to the cooperative Jahn-Teller effect in 3*d* or 4*f* electronic system of triplet ground state Γ_5 with the degeneracy of the quadrupolar moment. The triplet ground state Γ_5 of the charge fluctuation mode in Fig. 3 splits into the singlet state $\Delta\rho_{\rm order}$ in Fig. 4 and the excited doublets in the trigonal phase below T_c. It is expected that the charge ordering of the triplet Γ_5 mode at $T_c=292$ K in Yb_4As_3 releases the entropy of $\Delta S=R\ln3=9.13$ (J/mol K). The specific measurement[24] of Yb_4As_3, however, showed $\Delta S=0.3$ (J/mol K) around $T_c=292$ K, which is a considerably smaller amount than $R\ln3$ for the triplet ground state. It is possible that the short-range-order effect above the transition point T_c reduces the entropy around T_c. Furthermore, precise measurement of the specific heat is required to detect the latent heat associated with the first-order phase transition in Yb_4As_3. It is expected that other charge-fluctuation modes of Γ_1, Γ_2, and Γ_4 are excited states in Yb_4As_3. The observation of the excited state Γ_1, Γ_2, and Γ_4 in Yb_4As_3 is an important problem of spectroscopic measurements by optical methods.

The charge order $\Delta\rho_{\rm order}$ in Fig. 4 indicates clearly the linear chain alignment of Yb^{3+} ions along the body-diagonal [111] direction. This result based on the Landau theory is consistent with one-dimensional character of the magnetic excitation of Yb^{3+} ions at low temperatures in Yb_4As_3 observed by the neutron experiment.[8] The Yb^{3+} ions in $\Delta\rho_{\rm order}$ in Fig. 4 locates at the second nearest neighbor. As was pointed out by Lorenz,[25] the Madelung energy due to Coulomb interactions among the Yb^{3+} ions becomes minimum for the case that the Yb^{3+} ions locate at the third-nearest-neighbor sites. It should be noted that the charge-fluctuation mode of $\Delta\rho_{\rm Lornez}=3\rho_1-\rho_2-\rho_3-\rho_4-\rho_5+3\rho_6-\rho_7-\rho_8$ in the Lorenz model consist of Γ_4 representation, but does not contain Γ_5 representation. The Lorenz model, therefore, does not explain the structural phase transition from cubic T_d^6 to trigonal C_{3v}^6 associated with the charge ordering in Yb_4As_3. At the present stage it is not clear why the system favors the charge ordering $\Delta\rho_{\rm order}$ with Yb^{3+} alignment of the second nearest neighbor. It might be possible that the mixing effect between the *4f* state in Yb^{3+} ions and *p* state in As leads to energy gain for the linear alignment $\Delta\rho_{\rm order}$ in Fig. 4. The theory based on the band Jahn-Teller model succeeded in explaining the elastic softening of C_{44} and the trigonal distortion below T_c.[10] This means that the band Jahn-Teller model includes essentially the Coulomb interaction associated with the charge-fluctuation mode with Γ_5 symmetry discussed in the present paper.

In the present analysis we assumed the coexistence ratio of Yb^{3+} and Yb^{2+} ions to be 1 to 3 for the charge neutrality. This assumption is reasonable in Yb_4As_3 because of the extremely low carrier concentration of 0.1% in the molecular unit. The carrier increases considerably in the substituted system of $Yb_4(As_{1-x}Sb_x)_3$.[26] The screen effect by the carrier to the charge ordering in $Yb_4(As_{1-x}Sb_x)_3$ is an interesting subject for ultrasonic experiments. Actually the crossover from the charge order of the linear alignment of Yb^{3+} ions to the glass behavior reflecting the random distribution of Yb^{3+} ions have been observed by the ultrasonic measurements. The results will be published elsewhere. In the substitution compound of $Yb_4(As_{1-x}P_x)_3$, the carrier diminishes and semiconducting behavior appears at low temperatures.[27] The systematic investigation of the charge ordering in $Yb_4(As_{1-x}P_x)_3$ without the carrier is quite interesting when used to examine a screen effect to charge ordering of the system.

ACKNOWLEDGMENTS

The authors wish to thank A. Yoshihara, M. Kataoka, and B. Lüthi for valuable discussions on the Landau theory. The authors express their thanks to H. Harima for important information on the *International Tables for Crystallography*. This work was supported in part by the Grant-in-Aid for Scientific Research from the Ministry of Education, Science and Culture of Japan.

[1] A. Ochiai, T. Suzuki, and T. Kasuya, J. Phys. Soc. Jpn. **59**, 4129 (1990).
[2] T. Suzuki, Jpn. J. Appl. Phys., Part 1 **8**, 267 (1993).
[3] P. Bonville, A. Ochiai, T. Suzuki, and E. Vincent, J. Phys. I **4**, 595 (1994).
[4] S. Ono, J. G. Despault, L. D. Calvert, and J. B. Taylor, J. Less-Common Met. **22**, 51 (1970).
[5] M. Rams, K. Krolas, T. Tomola, A. Ochiai, and T. Suzuki, Hyperfine Interact. **97/98**, 125 (1996).
[6] A. Ochiai, Ph.D. thesis, Tohoku University, 1987.
[7] K. Iwasa, M. Kohgi, N. Nakajima, R. Yoshitake, Y. Hisazaki, H. Osumi, K. Tajima, N. Wakabayashi, Y. Haga, A. Ochiai, T. Suzuki, and A. Uesawa, J. Magn. Magn. Mater. **177-181**, 393 (1998).
[8] M. Kohgi, K. Iwasa, J.-M. Mignot, A. Ochiai, and T. Suzuki, Phys. Rev. B **56**, 388 (1997).
[9] P. Fulde, B. Schmidt, and P. Thalmeier, Europhys. Lett. **31**, 323 (1995).
[10] B. Schmidt, P. Thalmeier, and P. Fulde, Physica B **223&224**, 373 (1996).
[11] P. Fulde, Physica B **230-232**, 1 (1997).
[12] S. Suga, S. Ogawa, H. Namatame, M. Taniguchi, A. Kakizaki, T. Ishii, A. Fujimori, Se-Jung Oh, H. Kato, T. Miyahara, A. Ochiai, T. Suzuki, and T. Kasuya, J. Phys. Soc. Jpn. **58**, 4534 (1989).
[13] S. Kimuar, M. Ikezawa, A. Ochiai, and T. Suzuki, J. Phys. Soc. Jpn. **65**, 3951 (1996).
[14] H. Matsui, A. Ochiai, H. Harima, H. Aoki, T. Suzuki, T. Yasuda, and N. Toyota, J. Phys. Soc. Jpn. **66**, 3729 (1997).
[15] K. Takegahara and Y. Kaneta, J. Phys. Soc. Jpn. **60**, 4009 (1991).
[16] H. Harima, J. Phys. Soc. Jpn. **67**, 37 (1998).
[17] V. N. Antonov, A. N. Yaresko, A. Ta. Perlov, P. Thalmeier, P. Fulde, P. M. Oppeneer, and H. Eschrig, Phys. Rev. B **58**, 9752 (1998).
[18] T. Goto, Y. Nemoto, S. Nakamura, A. Ochiai, and T. Suzuki, Physica B **230-232**, 702 (1997).
[19] S. Nakamura, T. Goto, M. Kasaya, and S. Kunii, J. Phys. Soc. Jpn. **60**, 4311 (1991).
[20] The symmetry operators of T_d^6 in C. J. Bradley and A. P. Cracknell, *The Mathematical Theory of Symmetry in Solids* (Clarendon, Oxford, 1972) are introduced by the basic vectors $1/2(-a,a,a)$, $1/2(a,-a,a)$, $1/2(a,a,-a)$ of Bravais lattice Γ_c^v.
[21] T. Inui, Y. Tanabe, and Y. Onodera, *Group Theory and Its Applications in Physics* (Springer, Berlin, 1990).
[22] L. D. Landau and E. M. Lifshitz, *Statistical Physics* (Pergamon, Oxford, 1969).
[23] A. D. Bruce and R. A. Cowley, *Structural Phase Transitions* (Taylor & Francis, London, 1981).
[24] A. Ochiai, D. X. Li, Y. Haga, O. Nakamura, and T. Suzuki, Physica B **186-188**, 473 (1993).
[25] B. Lorenz, Phys. Status Solidi B **125**, 375 (1984).
[26] H. Aoki, A. Ochiai, T. Suzuki, R. Helfrich, and F. Steglich, Physica B **232**, 698 (1997).
[27] A. Ochiai, H. Aoki, T. Suzuki, R. Helfrich, and F. Steglich, Physica B **230-232**, 708 (1997).